Robust Decentralized Control of Inter-constrained Continuous Nonlinear Systems

A Receding Horizon Approach

ALEXANDROS FILOTHEOU

KTH Electrical Engineering

Master's Degree Project

Stockholm, Sweden February 2006

TRITA-EE 2006:666

Contents

Part I

Simulations

1

Introduction

The present part illustrates the efficacy of the advocated solutions, as described in chapters **??** and **??**, with regard to stabilization of multiple interconstrained agents, under the absence or presence of additive disturbances, in chapters 2 and 3 respectively.

The benefit of solving the problem this thesis addresses, as was formulated in chapter **??** and approached in chapters **??** and **??**, is that the procured solutions can be applied to a general class of likewise problems − the similarity relation relates to/the terms, the dynamic nature of the actors, and the structure of their habitat, but not the spirit of the problem itself.

All simulations were performed with the MATLAB NMPC routine provided with [1]. The source code of the simulations can be found on github[1].

[1] ??

1.1 The operational model

The simulacrum used for all agents in the following chapters shall be the three-dimensional model of the unicycle; its motion shall be expressed by the nonlinear continuous-time kinematic equations

$$\begin{aligned} \dot{x}(t) &= v(t)\cos\theta(t) \\ \dot{y}(t) &= v(t)\sin\theta(t) \\ \dot{\theta}(t) &= \omega(t) \end{aligned} \tag{1.1}$$

with $\mathbf{z} = [x, y, \theta]^\top$ the vector of states, $\mathbf{u} = [v, \omega]^\top$ the vector of inputs, and $\dot{\mathbf{z}} = f(\mathbf{z}, \mathbf{u})$ the (model) system's equation. We consider that $\mathbf{x} \in X$, $\mathbf{y} \in Y$ where $X \equiv Y \equiv \mathbb{R}$, $\theta \in \Theta \equiv (-\pi, \pi]$ and $\mathbf{u} \in \mathcal{U}$. In this 2D spatial environment, the obstacles of the workspace along with the workspace boundary itself assume an appropriately reformed form: that of a circle. The labeled space in which an arbitrary agent i moves, along with the spherical-obstacles-transformed to circles, is depicted in figure (1.1).

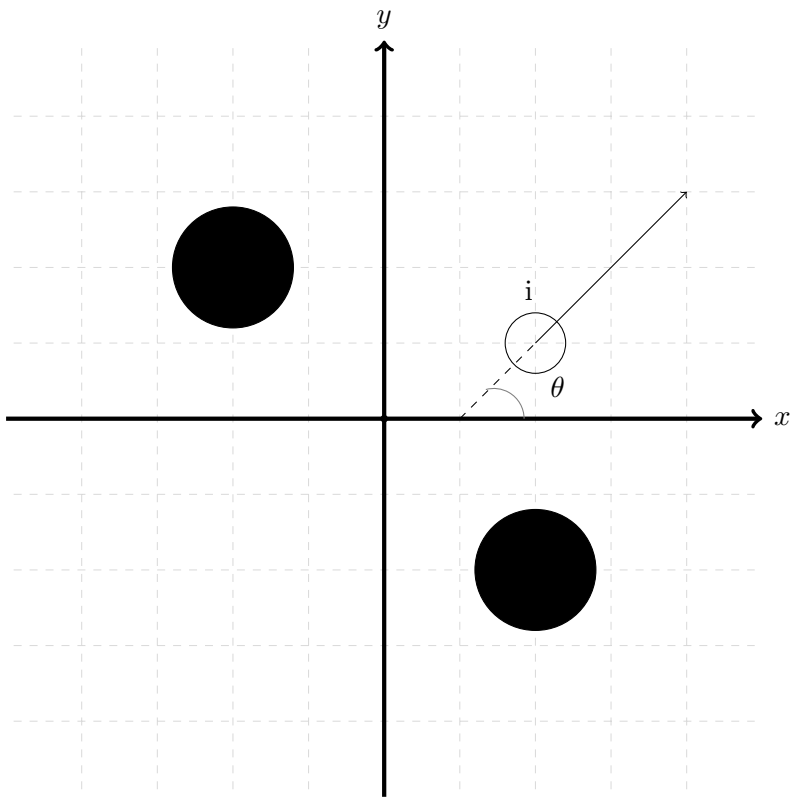

Figure 1.1: The 2D plane, agent i, whose orientation relative to the x axis is θ, and two obstacles.

The desired configuration shall be denoted by $\mathbf{z}_{des}$, the error dynamics by $\dot{\mathbf{e}} = g(\mathbf{e}, \mathbf{u})$ where $\mathbf{e}(t) = \mathbf{z}(t) - \mathbf{z}_{des}$ and $\mathbf{e} \in \mathcal{E} \equiv X \times Y \times \Theta \ominus \mathbf{z}_{des}$.

In the case were additive disturbances are considered, system (1.1) is expressed by

$$\begin{aligned} \dot{x}(t) &= v(t)\cos\theta(t) + \delta(t) \\ \dot{y}(t) &= v(t)\sin\theta(t) + \delta(t) \\ \dot{\theta}(t) &= \omega(t) + \delta(t) \end{aligned} \tag{1.2}$$

and its error dynamics are noted $\dot{\mathbf{e}} = g^R(\mathbf{e}, \mathbf{u})$ where $\mathbf{e}(t) = \mathbf{z}(t) - \mathbf{z}_{des}$ and $\mathbf{e} \in \mathcal{E} \equiv X \times Y \times \Theta \ominus \mathbf{z}_{des}$.

Lemma 1.1.1. Function g is Lipschitz continuous in $\mathcal{E} \times \mathcal{U}$ with a Lipschitz constant

$$L_g = v_{max}\sqrt{Q_{1,1} + Q_{1,2} + Q_{2,1} + Q_{2,2}}$$

where $\boldsymbol{Q} = Q_{\mu\nu}$ is the 3×3 matrix used to weigh the norms involved.

1.2 The problem reformed

Considering the conditions of the motivational problem as stated by problem (**??**), the reformed problem assumes the following form:

Problem 1.2.1. Assuming that

- all agents $i \in \mathcal{V}$ have access to their own and their neighbours' state and input vectors
- all agents $i \in \mathcal{V}$ have a (upper-bounded) sensing range d_i such that

$$d_i > \max\{r_i + r_j : \forall i, j \in \mathcal{V}, i \neq j\}$$

- at time $t = 0$ the sets $\mathcal{N}_i$ are known for all $i \in \mathcal{V}$ and $\sum_i |\mathcal{N}_i| > 0$
- at time $t = 0$ all agents are in a collision-free configuration with each other and the obstacles $\ell \in \mathcal{L}$
- All obstacles $\ell \in \mathcal{L}$ are situated in such a way that the distance between the two least distant obstacles is larger than the diameter of the agent with the largest diameter

the problem lies in procuring feasible controls for each agent $i \in \mathcal{V}$ such that for all agents and for all obstacles $\ell \in \mathcal{L}$ the following hold

1. Position and orientation configuration is achieved in steady-state $\mathbf{z}_{i,des}$

$$\lim_{t\to\infty} \|\mathbf{z}_i(t) - \mathbf{z}_{i,des}\| = 0$$

2. Inter-agent collision is avoided

$$\|\mathbf{p}_i(t) - \mathbf{p}_j(t)\| = d_{ij,a}(t) > \underline{d}_{ij,a}, \forall j \in \mathcal{V}\backslash\{i\}$$

   where $\mathbf{p}(t) = [x(t), y(t)]^\top$

3. Inter-agent connectivity loss between neighbouring agents is avoided

$$\|\mathbf{p}_i(t) - \mathbf{p}_j(t)\| = d_{ij,a}(t) < d_i, \forall j \in \mathcal{N}_i, \forall i : |\mathcal{N}_i| \neq 0$$

4. Agent-with-obstacle collision is avoided

$$\|\mathbf{p}_i(t) - \mathbf{p}_\ell(t)\| = d_{i\ell,o}(t) > \underline{d}_{i\ell,o}, \forall \ell \in \mathcal{L}$$

5. The control laws $\mathbf{u}_i(t)$ abide by their respective input constraints

$$\mathbf{u}_i(t) \in \mathcal{U}_i$$

for appropriate choice of constants $r_i, \mathbf{z}_{i,des}, \underline{d}_{ij,a}, d_i, \underline{d}_{i\ell,o}$ and neighbour sets $\mathcal{N}_i$, where $i \in \mathcal{V}$.

From the above we conclude that the constraint set $\mathcal{Z}_i$ for agent $i \in \mathcal{V}$ is

$$\begin{aligned}\mathcal{Z}_{i,t} = \big\{\mathbf{z}_i(t) \in X \times Y \times \Theta : \|\mathbf{p}_i(t) - \mathbf{p}_j(t)\| > \underline{d}_{ij,a}, \forall j \in \mathcal{R}_i(t),\\ \|\mathbf{p}_i(t) - \mathbf{p}_j(t)\| < d_i, \forall j \in \mathcal{N}_i,\\ \|\mathbf{p}_i(t) - \mathbf{p}_\ell\| > \underline{d}_{i\ell,o}, \forall \ell \in \mathcal{L},\\ -\pi < \theta_i(t) \leq \pi\big\}\end{aligned}$$

and the constraint set that corresponds to each agent for all $i \in \mathcal{V}$ is given by the Minkowski difference

$$\mathcal{E}_{i,t} = \mathcal{Z}_{i,t} \ominus \mathbf{z}_{i,des} \tag{1.3}$$

In the case of additive disturbances being considered, when each agent solves its own FHOCP, its constraint set $\mathcal{E}_i$ is replaced by a restricted constraint set that follows the same structure as (**??**).

The content of chapters 2 and 3 will demonstrate that agents $i \in \mathcal{V}$ can be stabilized when disturbances are absent, as demonstrated in chapter **??**, and, in the case where disturbances are present, that the magnitude of their errors about the equilibrium does not exceed a certain ceiling, as demonstrated in chapter **??**.

1.3 Simulation scenarios

The simulations were carried out under four different agents-obstacles configurations:

1. Two agents avoid one obstacle on their way to their steady-state configurations, without colliding with each other and without being separated by the obstacle (we demand that their distance is always smaller than the obstacle's diameter for the aim of cooperation).

2. Two agents pass through the space between two obstacles on their way to their steady-state configurations − again, the maximum allowed distance between the two agents is smaller than the diameter of the obstacle with the smallest radius.

3. Three agents avoid one obstacle on their way to their steady-state configurations, without colliding with each other and without being separated by the obstacle. In this case, two agents are (independently) neighbours of the third, that is, the third agent should maintain connectivity and avoid collision with both of the other two, but the latter will only have to avoid colliding with each other.

4. Three agents pass through the space between two obstacles on their way to their steady-state configurations. The conditions of this scenario assume those of points 2 and 3.

The four configurations are depicted in figures (1.2), (1.3), (1.4) and (1.5). Agent 1 is depicted in blue, agent 2 in red and agent 3 in yellow. The obstacles are depicted in black. A faint line connects neighbouring agents; it is coloured in green. Mark X denotes the desired position of an agent and its colour signifies the agent to be stabilized in that position.

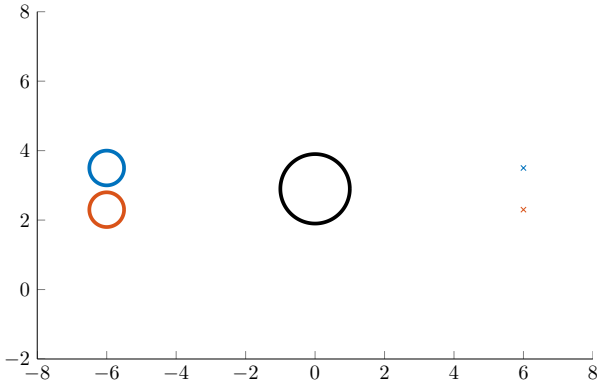

Figure 1.2: Test case one: two agents and one obstacle.

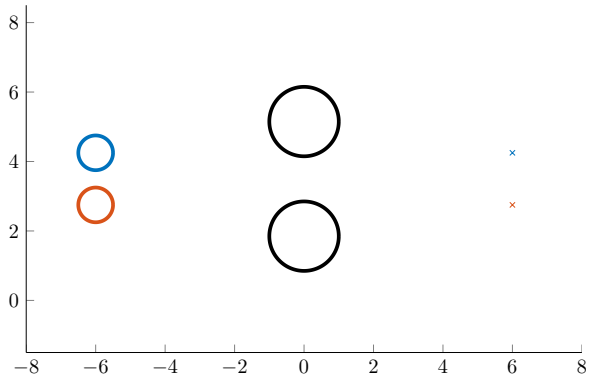

Figure 1.3: Test case two: two agents and two obstacles.

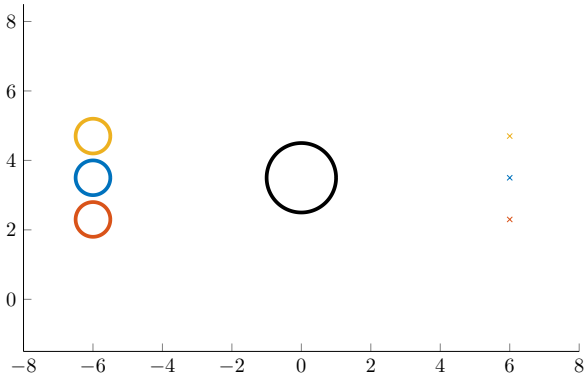

Figure 1.4: Test case three: three agents and one obstacle.

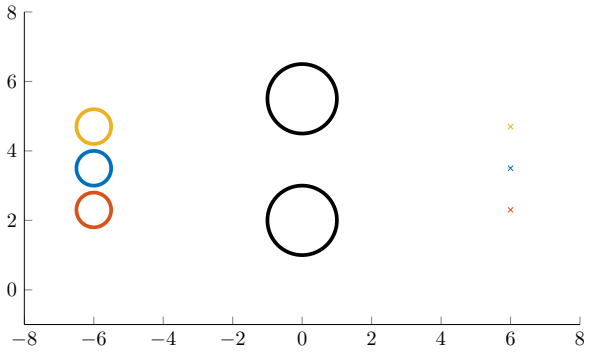

Figure 1.5: Test case four: three agents and two obstacles.

All configurations are as follows: the radius of all agents $i, j \in \mathcal{V}$ is $r_i = 0.5$; the radius of all obstacles is $r_\ell = 1.0$; the sensing range of all agents has a radius of $d_i = 4r_i + \epsilon = 2.0 + \epsilon$; the minimum distance between agents is $\underline{d}_{ij,a} = 2r_i + \epsilon = 1.0 + \epsilon$, and the minimum distance between agents and obstacles is $\underline{d}_{i\ell,o} = r_i + r_\ell + \epsilon = 1.5 + \epsilon$. ϵ was set to $\epsilon = 0.1$ in the disturbance-free cases and $\epsilon = 0.01$ in the cases where disturbances are present.

In the case of two agents, $\mathcal{V} = \{1, 2\}$, the neighbouring sets are $\mathcal{N}_1 = \{2\}$ and $\mathcal{N}_2 = \{1\}$, while in the case of three agents, $\mathcal{V} = \{1, 2, 3\}$, $\mathcal{N}_1 = \{2, 3\}$, $\mathcal{N}_2 = \{1\}$ and $\mathcal{N}_3 = \{1\}$.

Under the above configuration regime, all agents are constrained in bypassing the obstacle(s) from the same side, as they are prohibited from overtaking it (them) from different sides by the requirement that their sensing range be lower than the sum of the diameter of one obstacle and the radii of any two agents.

All simulations exhibit the translation of the visited theory into practice: in all test scenarios, all agents are successfully stabilized at, or about their desired configurations without their constraints being violated. Therefore, the next two chapters, instead of featuring all simulation results, will feature an anthology of the results pertaining to the most challenging task of those among the ones considered − that of three agents having to negotiate bypassing two obstacles while maintaining appropriate connectivity and avoiding collisions. A compre-

hensive collection of all simulation results is featured in appendices **??** and **??**. The individual initial and terminal configurations of each agent, the positions of the obstacles and various other parameters are reported in the appropriate sections.

2

Simulations of Disturbance-free Stabililization

The present chapter illustrates the stabilization of a group of agents whose motion dynamics are expressed by equations (1.1), and whose errors with respect to their respective steady-state configurations are constrained by the set found in equation (1.3). The control laws are designed as in chapter **??**.

In this setting, we consider the stabilization of three agents. Agent 1 is constrained in maintaining connectivity with agents 2 and 3 (and homologously vice-versa). All have to avoid colliding with each other and the with the obstacles in the workspace, and reach their desired configurations. The number of obstacles is two. The gap between them suffices for one agent to pass between them, but not for two or more.

2.1 Simulation results

The initial configurations of the three agents are $\mathbf{z}_1 = [-6, 3.5, 0]^\top$, $\mathbf{z}_2 = [-6, 2.3, 0]^\top$ and $\mathbf{z}_3 = [-6, 4.7, 0]^\top$. Their desired configurations in steady-state are $\mathbf{z}_{1,des} = [6, 3.5, 0]^\top$, $\mathbf{z}_{2,des} = [6, 2.3, 0]^\top$ and $\mathbf{z}_{3,des} = [6, 4.7, 0]^\top$. Obstacles o_1 and o_2 are placed between the two at $[0, 2.0]^\top$ and $[0, 5.5]^\top$ respectively. The penalty matrices $\boldsymbol{Q}$, $\boldsymbol{R}$, $\boldsymbol{P}$ were set to $\boldsymbol{Q} = 0.5(I_3 + 0.05\dagger_3)$, $\boldsymbol{R} = 0.005I_2$ and $\boldsymbol{P} = 0.5(I_3 + 0.05\dagger_3)$, where $\dagger_N$ is a $N \times N$ matrix whose elements are chosen at random between the values 0.0 and 1.0. The sampling time is $h = 0.1$ sec, the time-horizon is $T_p = 0.5$ sec, and the total execution time given was 3 sec.

Frames of the evolution of the trajectories of the three agents in the $x - y$ plane are depicted in figure (2.1). Here, the compound system avoids the pitfall of coming to a dead-end by having agent 1 act as a kind of mediator between the agents at the extremes as regards their trajectories: a too strict terminal penalty matrix $\boldsymbol{P}$, or an insufficient time-horizon length in relation to the maximum allowed input values, or a strongly diagonal structure for the penalty matrix $\boldsymbol{Q}$ could result in a situation where agent 1 is trapped between the two obstacles, with agents 2 and 3 following behind him, halted by the insufficient space between the two obstacles, and the geometry of the compound system resembling an isosceles triangle.

Once agent 3 clears the narrow, it is held up by agent 1, since their maximum allowed distance is tightly constrained. Agent 1 in turn has to make sure that its distance to agent 2 is within the allowed bounds as well. Figure (2.3) shows the evolution of the distance between agents 1 and 3 through time, and their abiding by the maximum-allowed-distance-between-agents constraint. The minimum and maximum allowed distances between the two agents are portrayed in the colour cyan.

Figure (2.4) shows the evolution of the distance between all agents and obstacle o_2 respectively, and, most crucially, it illustrates the fact that all agents avoid colliding with it. Figure (2.5) shows the input signals directing agent 1 through time. The minimum allowed distance between the agents and the obstacle, as well as the minimum and maximum allowed input sizes are portrayed in the colour cyan.

Figure (2.2) depicts the evolution of the error states of agent 1 through time. As the three error states converge to zero, the agent is stabilized at its desired 3D configuration.

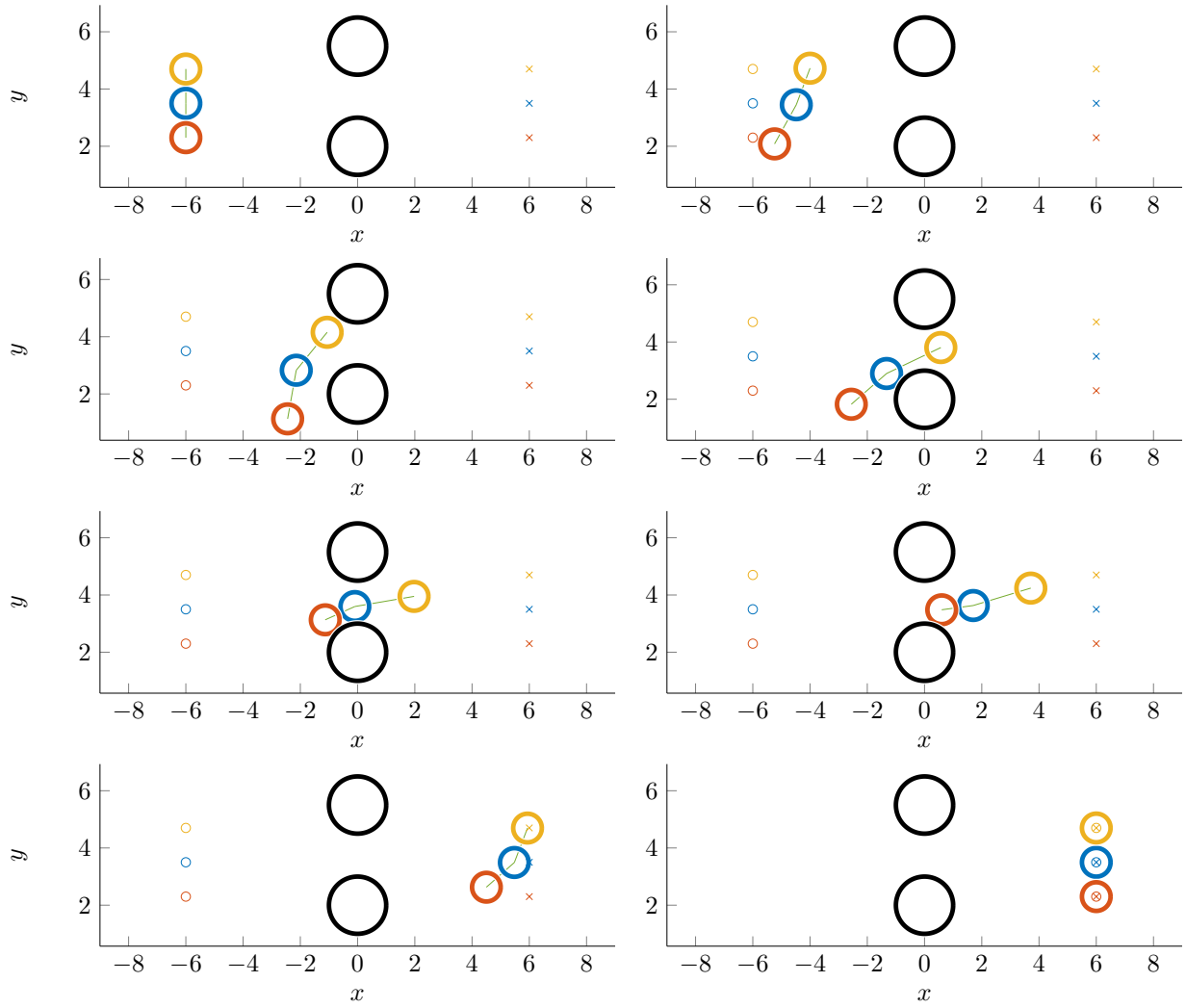

Figure 2.1: The trajectories of the three agents in the $x-y$ plane. Agent 1 is with blue, agent 2 with red and agent 3 with yellow. A faint green line connects agents deemed neighbours. The obstacles are black. Mark O denotes equilibrium configurations. Mark X marks desired configurations.

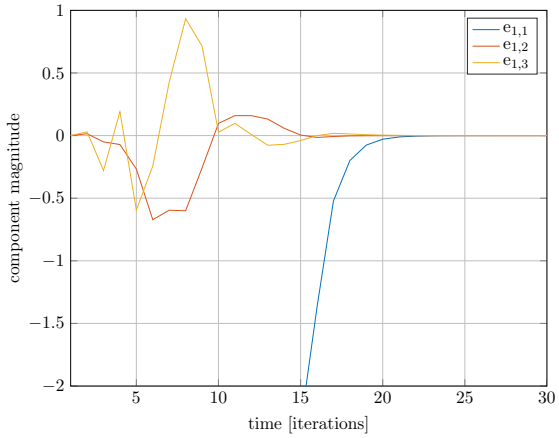

Figure 2.2: The evolution of the error states of agent 1 over time.

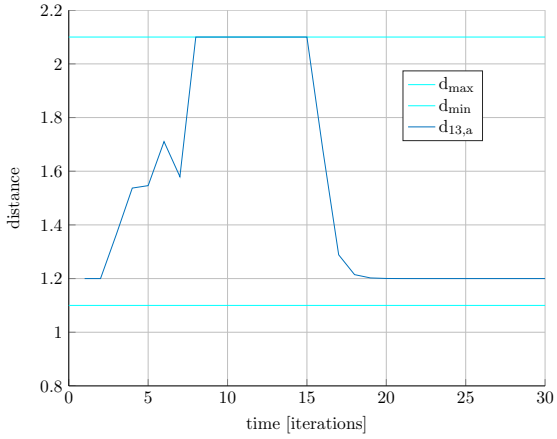

Figure 2.3: The distance between agents 1 and 3 over time. The maximum allowed distance has a value of 2.1 and the minimum allowed distance a value of 1.1.

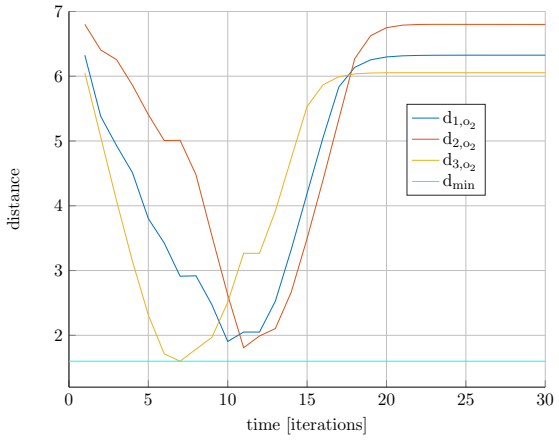

Figure 2.4: The distance between each agent and obstacle 2 over time. The minimum allowed distance has a value of 1.6.

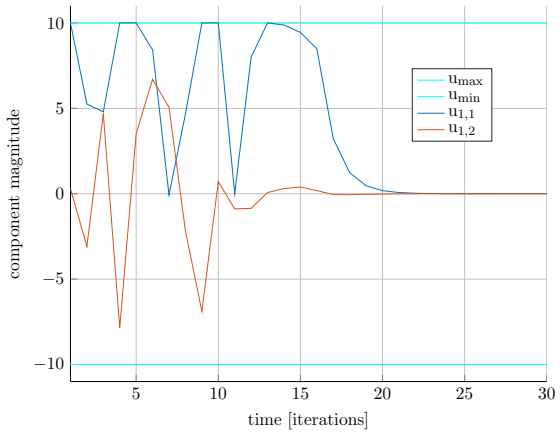

Figure 2.5: The inputs signals directing agent 1 over time. Their value is constrained between -10 and 10.

3

Simulations of Stabilization in the face of Disturbances

The present chapter illustrates the stabilization of a group of agents whose motion dynamics are expressed by equations (1.2), and whose errors with respect to their respective steady-state configurations are constrained by a restricted (compared to the unadulterated $\mathcal{E}_i$) constraint set, aiming at attenuating disturbances. The control laws are designed as in chapter **??**.

In this setting, we consider the stabilization of three agents. Agent 1 is constrained in maintaining connectivity with agents 2 and 3 (and homologously vice-versa). All have to avoid colliding with each other and the obstacles in the workspace, and reach their desired configurations under the pressure of being disturbed. The number of obstacles is two. The gap between them suffices for one agent to pass between them, but not for two or more.

3.1 Simulation results

In this case the initial configurations of the three agents are $\mathbf{z}_1 = [-6, 3.5, 0]^\top$, $\mathbf{z}_2 = [-6, 2.3, 0]^\top$ and $\mathbf{z}_3 = [-6, 4.7, 0]^\top$. Their desired configurations in steady-state are $\mathbf{z}_{1,des} = [6, 3.5, 0]^\top$, $\mathbf{z}_{2,des} = [6, 2.3, 0]^\top$ and $\mathbf{z}_{3,des} = [6, 4.7, 0]^\top$. Obstacles o_1 and o_2 are placed between the two at $[0, 2.0]^\top$ and $[0, 5.5]^\top$ respectively. The penalty matrices $\boldsymbol{Q}$, $\boldsymbol{R}$, $\boldsymbol{P}$ were set to $\boldsymbol{Q} = 0.7(I_3 + 0.5\dagger_3)$, $\boldsymbol{R} = 0.005I_2$ and $\boldsymbol{P} = 0.5(I_3 + 0.5\dagger_3)$, where $\dagger_N$ is a $N \times N$ matrix whose elements are chosen at random between the values 0.0 and 1.0. The sampling time is $h = 0.1$ sec, the time-horizon is $T_p = 0.5$ sec, and the total execution time given was 10 sec.

For compatibility with real situations, we assume that the disturbance signals affecting the agents are of the same nature (consider for instance the case of UAV's affected by wind); the disturbance signal considered was $\delta_i(t) = 0.1 * \sin 2t$ for all $i \in \mathcal{V} = \{1, 2, 3\}$. Therefore, $\overline{\delta}_i = 0.1$.

The evolution of the trajectories of the agents in the $x-y$ plane are omitted; they are (with minor variations) equivalent to those in the case where disturbances are absent. Figures (3.2) and (3.3) show the evolution of the distance between agents 1 and 3 through time, and the evolution of the distance between all agents and obstacle o_1 respectively. Figure (3.4) shows the input signals directing agent 2 through time. Just as in the case of absent disturbances, the compound system manages to clear the narrow between the two obstacles without agents colliding with each other or the obstacles, and in general, without violating any constraint present.

Figure (3.1) depicts the evolution of the error states of agent 1 through time. In contrast to the disturbance-free case, the error states do not converge to 0 at steady-state; rather, they oscillate periodically in accordance with the periodic nature of the disturbance, and in this case, with different amplitudes. Component-wise, the $y-$component exhibits the largest amplitude (the compound system oscillates in the vertical direction), however the largest effect of the disturbance is still being attenuated by a factor of 2: the peak-to-peak values of the $y-$component are approximately 0.1, which is half of the peak-to-peak value of the disturbance signal. For the $x-$ and $\theta-$components, the disturbance is attenuated by a factor of approximately 4.

Last but not at all least, figures (3.5) and (3.6) depict the evolution of the quadratic Lyapunov function $\mathbf{e}^\top \boldsymbol{P}\mathbf{e}$ through time for all three agents. Boundary values for the inputs and distances are portrayed in the colour cyan. The related constants concerned with the execution of this simulation are as follows: $L_{g_i} = 10.7354$, $L_{V_i} = 0.0471$, $\varepsilon_{\Psi_i} = 0.0654$ and $\varepsilon_{\Omega_i} = 0.0035$ for all $i \in \mathcal{V}$. The zoom-in'ed version of figure (3.5), figure (3.6), illustrates that once the energy measure of each agent (as measured by the Lyapunov function $V = \mathbf{e}^\top \boldsymbol{P}\mathbf{e}$) becomes lower than ε_Ψ (alternatively − when each system's trajectory enters set Ψ), it gets trapped below the value ε_Ω (and hence each system's trajectory is in turn trapped inside the terminal set Ω) in finite time, and does not exit it.

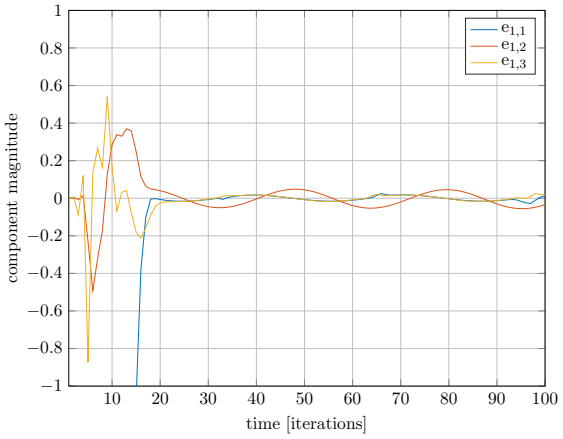

Figure 3.1: The evolution of the error states of agent 1 over time.

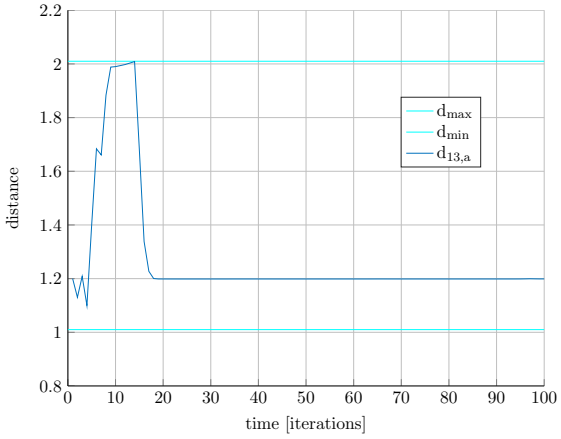

Figure 3.2: The distance between agents 1 and 3 over time. The maximum allowed distance has a value of 2.01 and the minimum allowed distance a value of 1.01.

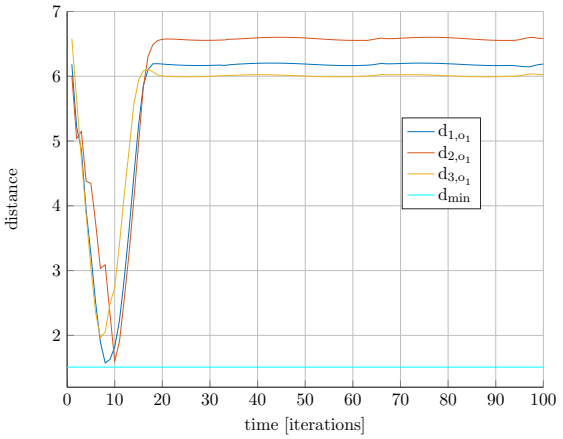

Figure 3.3: The distance between each agent and obstacle 1 over time. The minimum allowed distance has a value of 1.51.

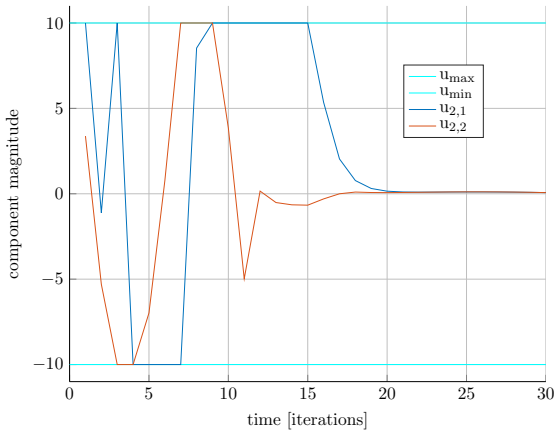

Figure 3.4: The inputs signals directing agent 2 over time. Their value is constrained between −10 and 10.

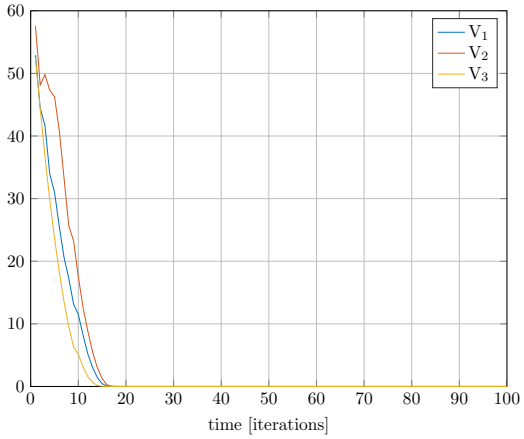

Figure 3.5: The $\boldsymbol{P}-$norms of the errors of the three agents through time.

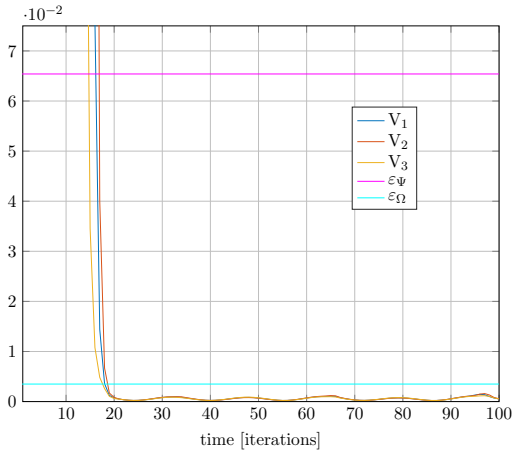

Figure 3.6: The $\boldsymbol{P}-$norms of the errors of the three agents through time, focused. The colour magenta is used to illustrate the threshold $\mathcal{E}_\Psi$, while cyan is used for $\mathcal{E}_\Omega$.

Bibliography

[1] L. Grüne and J. Pannek, *Nonlinear Model Predictive Control: Theory and Algorithms*. Communications and Control Engineering, Springer International Publishing, 2016.